

# Role of the Surface-Exposed and Copper-Coordinating Histidine in Blue Copper Proteins: The Electron-Transfer and Redox-Coupled Ligand Binding Properties of His117Gly Azurin

Lars J. C. Jeuken,<sup>†</sup> Pieter van Vliet,<sup>†</sup> Martin Ph. Verbeet,<sup>†</sup> Raul Camba,<sup>§</sup>  
James P. McEvoy,<sup>§</sup> Fraser A. Armstrong,<sup>§</sup> and Gerard W. Canters<sup>\*,†</sup>

Contribution from the Leiden Institute of Chemistry, Leiden University, P.O. Box 9502, 2300 RA, Leiden, The Netherlands, and Department of Chemistry, Inorganic Chemistry Laboratory, Oxford University, South Parks Road, Oxford, OX1 3QR, England

Received February 21, 2000

**Abstract:** In many reduced blue copper proteins the C-terminal surface-exposed active-site histidine protonates at low pH and dissociates from the Cu atom. In this state, the proteins exhibit high reduction potentials and low oxidation rates. In contrast, the homologous histidine (117) of azurin does not protonate. This difference has been examined by studying the electrochemical behavior of an azurin mutant in which histidine 117 is replaced by glycine to create a cavity enabling external ligands to enter the protein and coordinate to the Cu. We show that the external ligands influence the electrochemical properties of the copper site, as studied with potentiometric titrations of protein solutions and with fast-scan and low-temperature cyclic voltammetry of protein films adsorbed on graphite electrodes. The reduction potential ( $E^0$ ) of His117Gly azurin without external ligands is very high, at  $670 \pm 10$  mV, but it decreases upon addition of  $\text{Cl}^-$  or imidazole. The reduced form has little affinity for these ligands; however, under fast-scan or cryoscopic conditions ( $-70$  °C, 70% methanol) the reduced form of the imidazole complex can be “trapped”, and a reversible redox couple is established. The electrochemical kinetics of the trapped state are very fast and similar to those of wild-type (*wt*) azurin. The reduction potential is  $\sim 60$  mV lower than for *wt* azurin under identical conditions. The dissociation constant  $K_{\text{diss}}$  of the Cu(I)–imidazole complex lies between 14 and 69 M at 20 °C, while that of the Cu(I)– $\text{Cl}^-$  complex is estimated to be as high as  $10^6$  M. These very low affinities show that for *wt* azurin the covalent link between the imidazole side chain of His117 and the protein framework is crucial for maintaining this side chain as a ligand of the Cu(I) ion.

## Introduction

Small blue copper proteins (9–14 kDa) are a class of mononuclear copper proteins that contain a so-called type-1 or “blue” copper site and function in electron transfer. Type-1 copper sites exhibit several distinguishing spectroscopic characteristics, which include an intense absorption band near 600 nm ( $\epsilon = 3000\text{--}6000 \text{ M}^{-1} \text{ cm}^{-1}$ ) arising from a (Cys)S  $\rightarrow$  Cu(II) charge-transfer transition, and a small hyperfine splitting in the  $g_{\parallel}$  region ( $A_{\parallel} < 100 \times 10^{-4} \text{ cm}^{-1}$ ) of their EPR spectra<sup>1</sup>.

For a number of blue copper proteins, such as azurin,<sup>2–5</sup> plastocyanin,<sup>6</sup> and amicyanin,<sup>7,8</sup> the 3D structure has been solved. From these structures a prototypical type-1 copper site

emerges, in which the copper ion is strongly coordinated by the  $S^{\gamma}$  of a cysteine and the  $N^{\delta}$ 's of two histidines. This  $N_2S$  donor set is conserved in all members of the blue copper protein family. A less conserved ligand, the  $S^{\delta}$  of a methionine, serves as an axial group. Azurin is unique among the blue copper proteins in that it contains a second axial group, the carbonyl oxygen of a glycine.

Crystal structures indicate that the copper sites are very similar in oxidized and reduced states<sup>6,9,10</sup> and, as a consequence, the reorganization energies are low.<sup>11,12</sup> This makes the blue copper sites suitable for fast electron transfer. At low pH, however, a conformational change not seen in azurin is observed in the reduced copper sites of the blue copper proteins amicyanin, plastocyanin, and pseudoazurin.<sup>6,10,13</sup> The  $N^{\delta}$  of the surface-exposed histidine protonates and dissociates from the Cu atom. Crystal structures and EXAFS studies at different pH values have shown that the Cu(I) moves into the plane of the remaining ligands—a cysteine, a histidine, and a methionine.<sup>6,10,13</sup> In this

\* Author for correspondence. Professor Dr. G. W. Canters, Leiden Institute of Chemistry, Leiden University, Gorlaeus Laboratories, P.O. Box 9502, 2300 RA Leiden, The Netherlands, Telephone: (+31)71-5274339. Fax: (+31)71-5274349. E-mail: canters@chem.leidenuniv.nl.

<sup>†</sup> Leiden Institute of Chemistry.

<sup>§</sup> Oxford University.

(1) Solomon, E. I.; Baldwin, M. J.; Lowery, M. D. *Chem. Rev.* **1992**, 92, 521–542.

(2) Nar, H.; Messerschmidt, A.; Huber, R.; van de Kamp, M.; Canters, G. W. *J. Mol. Biol.* **1991**, 221, 765–772.

(3) Adman, E. T.; Stenkamp, R. E.; Sieker, L. C.; Jensen, L. H. *J. Mol. Biol.* **1978**, 123, 35–47.

(4) Adman, E. T.; Jensen, L. H. *Isr. J. Chem.* **1981**, 21, 8–12.

(5) Baker, E. N. *J. Mol. Biol.* **1988**, 203, 1071–1095.

(6) Guss, J. M.; Harrowell, P. R.; Murata, M.; Norris, V. A.; Freeman, H. C. *J. Mol. Biol.* **1986**, 192, 361–387.

(7) Kalverda, A. P.; Wymenga, S. S.; Lommen, A.; van de Ven, F. J.; Hilbers, C. W.; Canters, G. W. *J. Mol. Biol.* **1994**, 240, 358–371.

(8) Romero, A.; Nar, H.; Huber, R.; Messerschmidt, A.; Kalverda, A. P.; Canters, G. W.; Durley, R. C.; Mathews, F. S. *J. Mol. Biol.* **1994**, 236, 1196–1211.

(9) Shepard, W. E. B.; Anderson, B. F.; Lewandoski, D. A.; Norris, G. E.; Baker, E. N. *J. Am. Chem. Soc.* **1990**, 112, 7817–7819.

(10) Vakoufari, E.; Wilson, K. S.; Petratos, K. *FEBS Lett.* **1994**, 347, 203–206.

(11) Malmström, B. G. *Eur. J. Biochem.* **1994**, 223, 711–718.

(12) Williams, R. J. P. *Eur. J. Biochem.* **1995**, 234, 363–381.

(13) Lommen, A.; Pandya, K. I.; Koningsberger, D. C.; Canters, G. W. *Biochim. Biophys. Acta* **1991**, 1076, 439–447.

state, the blue copper sites exhibit increased reduction potentials and show diminished oxidation rates when reacting with small inorganic oxidants.<sup>14–16</sup> Consequently, this state is sometimes referred to as “redox inactive”.

To find out why azurin does not exhibit this conformational change and to establish the role of the C-terminal histidine ligand in determining the redox and kinetic properties of blue copper sites, we studied the dynamic electrochemical properties of a blue copper protein mutant, His117Gly azurin, in which the histidine that normally dissociates and protonates in other blue copper proteins is replaced by glycine. Previously we showed that in this variant the copper ion is accessible to exogenous ligands.<sup>17–19</sup> Depending on the kind of ligand, different types of copper sites are obtained: binding of Cl<sup>-</sup>, Br<sup>-</sup>, imidazole (and imidazole derivatives), and pyridine (and pyridine derivatives) restores the spectroscopic features that are characteristic of the type-1 copper sites, whereas water, histidine, or histamine create novel azurin copper sites with spectroscopic features that are more similar to “normal” or type-2 copper sites. For example, without external ligands, His117Gly azurin is green with absorption maxima at 420 and 628 nm, but addition of imidazole restores the blue color of *wt* azurin (main absorption at 626 nm, cf. *wt* azurin, 628 nm) and other characteristic spectroscopic features such as are observed by EPR, ENDOR, resonance Raman, and EXAFS.<sup>17,18,20,21</sup> The results imply that the structure of the mutant protein and the position of the remaining ligands are maintained despite replacement of the histidine.

In this study we report on the redox properties of His117Gly azurin, as studied by potentiometric titrations and by protein-film cyclic voltammetry carried out in both fast-scan and cryoscopic modes.<sup>22,23</sup> The experiments reveal the redox-coupled ligand exchange properties of two external ligands, that is, chloride and imidazole, at the Cu site in His117Gly azurin. Imidazole was studied since it best restores the *wt* azurin spectroscopic features in His117Gly azurin, while chloride represents the group of simple anions that are also able to restore type-1 characteristics.<sup>18</sup> The voltammetric studies overcome the problems caused by the high lability of these systems; most significantly, the results show that imidazole ligation restores the redox properties of *wt* azurin, in particular its capability for fast electron transfer.

## Materials and Methods

**Proteins.** A sample of the His117Gly variant of *Pseudomonas aeruginosa* azurin was obtained as described previously.<sup>24</sup> The protein was isolated in its apo-form, and Cu(NO<sub>3</sub>)<sub>2</sub> was supplemented shortly before the experiments. Subsequently, the protein was incubated for 20–30 min at room temperature under anaerobic conditions,<sup>25</sup> which were obtained by extensive flushing with argon. The concentration of

apo-protein was determined from the observed absorbance at 280 nm and the corresponding extinction coefficient  $\epsilon_{280}$ . On the basis of the extinction at 420 nm (see results section),  $\epsilon_{280}$  values for apo- and oxidized holo-proteins were calculated as  $9.1 \pm 0.1$  and  $9.7 \pm 0.1$  mM<sup>-1</sup> cm<sup>-1</sup>, respectively. Unless indicated otherwise, the experiments were performed at 20 °C in 20 mM 2-[*N*-morpholino]ethanesulfonic acid (MES, Sigma) pH 6.0.

**Optical Spectroscopy (UV–Vis Adsorption).** Optical spectra were recorded at 298 K on a Shimadzu UV-2101PC UV–vis spectrometer. The spectra were analyzed using the Personal Spectroscopy Software UV-2101PC version 3 of Shimadzu.

**Extinction Coefficients and Ligand Affinity.** Small aliquots of Cu(NO<sub>3</sub>)<sub>2</sub> (Merck) were added to the apo-form of His117Gly azurin (~0.05–0.1 mM) either in the absence or presence of excess external ligand (i.e., 5 mM imidazole (99%, Acros) or 1.0 M NaCl (Merck)). Optical spectra were then recorded, and the titration slopes (absorbance versus copper concentration) were used to determine the extinction coefficients and binding constants.

In a second experiment, small aliquots of ligands (i.e., chloride or imidazole) were added to His117Gly azurin (~0.05–0.1 mM) reconstituted with ~0.8 equiv of Cu(NO<sub>3</sub>)<sub>2</sub>, and optical spectra were recorded. The stock solutions containing the ligands in 20 mM MES were adjusted to pH 6.0 prior to the experiments using NaOH or H<sub>2</sub>SO<sub>4</sub>. Absorbance data were analyzed by least-squares fitting to obtain dissociation constants of the protein/ligand complexes. All titrations were performed under anaerobic conditions, which were maintained by continuously flushing with argon.

**Potentiometric Titrations.** For the potentiometric titrations an “anaerobic” cell was constructed to measure UV–vis spectra at equilibrated electrode potentials. It featured a quartz cuvette adapted with three top-mounted “fingers”, two of which were used to insert reference and Pt counter electrodes, with the third being used to flush the cell with Ar. The saturated Hg/Hg<sub>2</sub>SO<sub>4</sub> reference electrode (Radiometer, Denmark) was calibrated with quinhydrone (Sigma). All potentials are quoted versus the standard hydrogen electrode (SHE) with  $E_{\text{ref,electrode}} = 460$  mV vs SHE.

To reconstitute apo-His117Gly azurin, ~1.2 equiv of Cu(II) were added, followed where required by the ligands (i.e., imidazole/H<sub>2</sub>SO<sub>4</sub> at pH 6.0, or chloride). The amount of oxidized protein during these titrations was determined spectrophotometrically. To suppress the occurrence of more than one species of the oxidized protein in the solution, only saturating ligand concentrations were used (>95% bound ligand in the oxidized form). For imidazole, 5 mM was sufficient, while for chloride, saturation required concentrations greater than 0.5 M (see results). After 30 min the mediators (i.e., ferricyanide (Fluka), 1,2-ferrocene dicarboxylic acid (Sigma) and, in the case of the titrations involving chloride, sodium hexachloroiridate(IV) (Na<sub>2</sub>IrCl<sub>6</sub>, Aldrich)) were added, typically at ratios between 1:100 and 1:20 with respect to the protein concentration (0.1–0.2 mM).

The potentials and the optical spectra of the protein solutions (0.1–0.2 mM) were measured while reducing the sample stepwise with aliquots of ascorbic acid, allowing the spectrum to stabilize at each stage. A “reverse” titration was performed to check for drifts in potential or non-equilibrium conditions. Reoxidation of His117Gly azurin was achieved with Na<sub>2</sub>IrCl<sub>6</sub> ( $E^{\circ} = 0.867$  mV<sup>26</sup>) when chloride was used as the external ligand, or by K<sub>3</sub>Fe(CN)<sub>6</sub> ( $E^{\circ} \approx 0.41$  mV<sup>26,27</sup>) when imidazole (100 mM or 250 mM) was used. All potentiometric titrations were performed in 20 mM MES, pH 6.0 with 33 mM Na<sub>2</sub>SO<sub>4</sub> at 20 °C.

The imidazole titrations on “redox” buffered His117Gly azurin were performed on a solution containing an exact quantity of His117Gly azurin (~0.1 mM), 4 mM 1:1 ferri/ferrocyanide, in 100 mM MES at pH 6.0. Imidazole was added from a stock solution, which was adjusted

- (14) Lommen, A.; Canters, G. W. *J. Biol. Chem.* **1990**, *265*, 2768–2774.  
 (15) DiBilio, A. J.; Dennison, C.; Gray, H. B.; Ramirez, B. E.; Sykes, A. G.; Winkler, J. R. *J. Am. Chem. Soc.* **1998**, *120*, 7551–7556.  
 (16) Sykes, A. G. *Chem. Soc. Rev.* **1985**, *14*, 283–315.  
 (17) den Blaauwen, T.; Hoitink, C. W.; Canters, G. W.; Han, J.; Loehr, T. M.; Sanders-Loehr, J. *Biochemistry* **1993**, *32*, 12455–12464.  
 (18) den Blaauwen, T.; Canters, G. W. *J. Am. Chem. Soc.* **1993**, *115*, 1121–1129.  
 (19) Kroes, S. J.; Salgado, J.; Parigi, G.; Luchinat, C.; Canters, G. W. *J. Biol. Inorg. Chem.* **1996**, *1*, 551–559.  
 (20) van Gastel, M.; Coremans, J. W. A.; Jeuken, L. J. C.; Canters, G. W.; Groenen, E. J. *J. Phys. Chem. A* **1998**, *102*, 4462–4470.  
 (21) Coremans, J. W. A.; van Gastel, M.; Poluektov, O. G.; Groenen, E. J. J.; den Blaauwen, T.; van Pouderoyen, G.; Canters, G. W.; Nar, H.; Hammann, C.; Messerschmidt, A. *Chem. Phys. Lett.* **1995**, *235*, 202–210.  
 (22) McEvoy, J. P.; Armstrong, F. A. *Chem. Commun.* **1999**, 1635–1636.  
 (23) Hirst, J.; Armstrong, F. A. *Anal. Chem.* **1998**, *70*, 5062–5071.  
 (24) den Blaauwen, T.; van de Kamp, M.; Canters, G. W. *J. Am. Chem. Soc.* **1991**, *113*, 5050–5052.

(25) Anaerobic conditions were necessary since the copper site of the His117Gly mutant is air-sensitive. Crystal structures have revealed that the S<sup>γ</sup> of the cysteine is susceptible to oxidation. See: Hammann, C.; van Pouderoyen, G.; Nar, H.; Gomis, R. F.; Messerschmidt, A.; Huber, R.; den Blaauwen, T.; Canters, G. W. *J. Mol. Biol.* **1997**, *266*, 357–366.

(26) *Handbook of Chemistry and Physics*; CRC Press: Boston, 1992; pp 8–19.

(27) O'Reilly, J. E. *Biochim. Biophys. Acta* **1973**, *292*, 509–515.

to pH 6.0 with H<sub>2</sub>SO<sub>4</sub> before the titration. The concentration of oxidized His117Gly azurin was determined from the absorbance at 628 nm,  $A_\lambda$ , given by

$$A_\lambda = \epsilon_\lambda^{\text{nl}}[\text{H117G}^{\text{ox}}] + \epsilon_\lambda^{\text{Im}}[\text{H117G}^{\text{ox}}/\text{Im}]$$

The reduction potential (vs the redox buffer),  $E^{\text{O}}(\text{Im})$ , was calculated from the Nernst equation

$$E = E^{\text{O}}(\text{Im}) + \frac{RT}{nF} \ln \left( \frac{[\text{H117G}^{\text{ox}}] + [\text{H117G}^{\text{ox}}/\text{Im}]}{[\text{H117G}^{\text{red}}] + [\text{H117G}^{\text{ox}}/\text{Im}]} \right)$$

Here H117G/Im and H117G represent azurin species in which the Cu is and is not complexed by imidazole, respectively, the superscripts ox and red denote the oxidized and reduced species,  $\epsilon_\lambda^{\text{nl}}$  and  $\epsilon_\lambda^{\text{Im}}$  represent the extinction coefficients at  $\lambda$  nm of oxidized His 117Gly and His117Gly/Im azurin, respectively, and  $E$  is the potential of the redox buffer.

Successive additions of imidazole to the “redox-buffer” changed the reduction potential of ferricyanide due to the increase in ionic strength,<sup>27</sup> making it necessary to correct the potential at each imidazole concentration. For this, the reduction potentials of ferricyanide at increasing imidazole concentrations were determined by cyclic voltammetry in separate experiments.

**Fast-Scan Protein-Film Voltammetry.** For the fast-scan experiments, the apo-form of His117Gly azurin was reconstituted with approximately 0.8 equiv of Cu(NO<sub>3</sub>)<sub>2</sub> and subsequently incubated with imidazole (5 mM) or NaCl (0.5 M) (each with 20 mM MES pH 6.0). The pyrolytic graphite edge (PGE) working electrode (graphite obtained from Advanced Ceramics Corporation, Wales) was polished with diamond polish (Aerosol diamond, 3 or 6 micrometers purchased from Kemet) on a cloth, washed with water, and then sonicated. To form a film, protein solution was applied to the electrode surface using a Pasteur pipet that had been drawn to a fine tip with a flame. Excess liquid was drawn back into the pipet tip, and the wet electrode was inserted promptly into the cell. Scans at 0 °C were recorded in a cell solution consisting of 250 mM imidazole, 20 mM MES, 150 mM Na<sub>2</sub>SO<sub>4</sub>, and 2 mM neomycin, adjusted to pH 6.0 with H<sub>2</sub>SO<sub>4</sub>. Scans with Cl<sup>-</sup> as an external ligand were performed at 20 °C with different concentrations of NaCl in 20 mM MES, pH 6.0, and 2 mM neomycin. For concentrations of NaCl below 0.1 M, the ionic strength of the buffer solution was adjusted to 0.1 M with Na<sub>2</sub>SO<sub>4</sub>. Neomycin is a coadsorbent, which stabilizes the protein film (ideally up to monolayer coverage) on the electrode.

The electrochemical cells were constructed as described before.<sup>28,29</sup> Analogue cyclic voltammetry was recorded using an Autolab electrochemical analyzer (Eco-chemie, Utrecht, The Netherlands) equipped with a PGSTAT 20 potentiostat and a fast analogue scan generator in combination with a fast AD converter (ADC750). Voltammograms were Fourier-filtered; then background (electrode) current subtraction was performed with a program (written by Dr H. A. Heering) which fits a cubic spline function<sup>30</sup> to the baseline in regions sufficiently far from the peak and extrapolates it throughout the peak region.

**Cryovoltammetry.** Cyclic voltammograms at -70 °C were recorded in 70% methanol, 20 mM imidazole, 20 mM MES, 100 mM NaClO<sub>4</sub>, 0.2 mM neomycin at pH\* 6.0 (as measured at 0 °C) after establishing a protein film under aqueous conditions. The experimental method was based on that described previously.<sup>22</sup> Analogue cyclic voltammetry and data handling were performed as described in the section on fast-scan protein-film voltammetry.

## Theory

**Ligand affinity.** Binding of imidazole to His117Gly<sup>ox</sup> azurin,  $[\text{H117G}^{\text{ox}}] + [\text{Im}] \rightleftharpoons [\text{H117G}^{\text{ox}}/\text{Im}]$  with dissociation constant

(28) Hirst, J.; Duff, J. C.; Jameson, G. N. L.; Kemper, M. A.; Burgess, B. K.; Armstrong, F. A. *J. Am. Chem. Soc.* **1998**, *120*, 7085–7094.

(29) Hirst, J.; Duff, J. C.; Jameson, G. N. L.; Kemper, M. A.; Burgess, B. K.; Armstrong, F. A. *J. Am. Chem. Soc.* **1998**, *120*, 13284

(30) Press: W. H.; Flannery, B. P.; Teukolsky, S. A.; Vetterling, W. T. *Numerical Recipes in Pascal*; Cambridge University Press: New York, 1989;

$K_{\text{ox}}^{\text{Im}}$ , is in competition with the reaction  $[\text{Im}] + [\text{H}^+] \rightleftharpoons [\text{Im} \cdot \text{H}^+]$  with dissociation constant  $K_a$ . The concentration of the H117G<sup>ox</sup>/Im complex at different total imidazole concentrations is therefore given by

$$[\text{H117G}^{\text{ox}}/\text{Im}]^2 - \{[\text{H117G}^{\text{ox}}]_t + [\text{Im}]_t + K_{\text{ox,asp}}^{\text{Im}}\} \times [\text{H117G}^{\text{ox}}/\text{Im}] + [\text{H117G}^{\text{ox}}]_t \times [\text{Im}]_t = 0 \quad (1A)$$

in which  $[\text{H117G}^{\text{ox}}]_t$  and  $[\text{Im}]_t$  represent the total concentrations of oxidized His117Gly azurin and added imidazole in solution, respectively,

$$[\text{H117G}^{\text{ox}}]_t \equiv [\text{H117G}^{\text{ox}}/\text{Im}] + [\text{H117G}^{\text{ox}}]$$

$$[\text{Im}]_t \equiv [\text{H117G}^{\text{ox}}/\text{Im}] + [\text{Im}] + [\text{Im} \cdot \text{H}^+]$$

and  $K_{\text{ox,app}}^{\text{Im}}$  is the apparent dissociation constant. Knowing the  $\text{p}K_a$  of the imidazole ligand (6.95 at 25 °C<sup>31</sup>) the apparent dissociation constant ( $K_{\text{ox,app}}^{\text{Im}}$ ) of the His117Gly/Im complexed can be related to the real dissociation constant ( $K_{\text{ox}}^{\text{Im}}$ ) by:<sup>32</sup>

$$K_{\text{ox,app}}^{\text{Im}} \equiv \frac{([\text{Im}] + [\text{ImH}^+]) \times [\text{H117G}^{\text{ox}}]}{[\text{H117G}^{\text{ox}}/\text{Im}]} \quad (1B)$$

with

$$\log \alpha \equiv \text{p}K_a - \text{pH}$$

and

$$K_{\text{ox}}^{\text{Im}} \equiv \frac{[\text{Im}] \times [\text{H117G}^{\text{ox}}]}{[\text{H117G}^{\text{ox}}/\text{Im}]}$$

**Reduction Potentials.** Combining the dissociation constants of reduced and oxidized His117Gly azurin with the Nernst equation results in eq 2.<sup>33</sup> Here,  $E^{\text{O}}_{\text{nl}}$  is the reduction potential in the absence of imidazole,  $R$  is the gas constant,  $T$  is the temperature,  $n$  is the number of electrons transferred (=1),  $F$  is the Faraday constant, and  $[\text{Im}]$  denotes the (unprotonated) imidazole concentration:

$$E^{\text{O}}(\text{Im}) = E^{\text{O}}_{\text{nl}} - \frac{RT}{nF} \ln \left( \frac{K_{\text{red}}^{\text{Im}}(K_{\text{ox}}^{\text{Im}} + [\text{Im}])}{K_{\text{ox}}^{\text{Im}}(K_{\text{red}}^{\text{Im}} + [\text{Im}])} \right) \quad (2)$$

Substituting  $[\text{Im}]$  by  $[\text{Im}] = ([\text{Im}] + [\text{ImH}^+])/(1 + \alpha)$  and setting  $[\text{Im}] + [\text{ImH}^+]$  equal to  $[\text{Im}]_t$ , which is a valid approximation under the conditions of the experiment, that is, when the total concentration of imidazole is in great excess over the total concentration of His117Gly, we obtain

$$E^{\text{O}}(\text{Im}) = E^{\text{O}}_{\text{nl}} - \frac{RT}{nF} \ln \left( \frac{K_{\text{red,app}}^{\text{Im}}(K_{\text{ox,app}}^{\text{Im}} + [\text{Im}]_t)}{K_{\text{ox,app}}^{\text{Im}}(K_{\text{red,app}}^{\text{Im}} + [\text{Im}]_t)} \right) \quad (3)$$

## Results

**Ligand Affinity.** In the absence of external ligands, His117Gly azurin (pH 6.0) displays absorption maxima at 420 and 628

(31) Merck Catalog. See <http://www.merck.de>.

(32) Williams, R. J. P.; Frausto da Silva, J. J. R. *The Natural Selection of the Chemical Elements*; Clarendon Press: Oxford, 1996; pp 169–171.

(33) Moore, G. R.; Pettigrew, G. W. *Cytochromes c. Evolution, Structural and Physicochemical Aspects*; Springer-Verlag: Berlin, Heidelberg, 1990; pp 314–315.



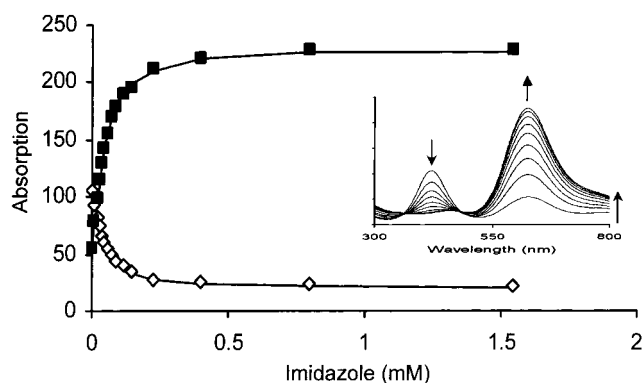


**Figure 1.** The absorbances ( $\times 1000$ ) at 628 nm ( $\blacksquare$ ) and 420 nm ( $\diamond$ ) of His117Gly azurin ( $\sim 50 \mu\text{M}$ , 20 mM MES, pH 6.0, 20 °C) as a function of the total imidazole concentration. The lines represent least-squares fits according to equation (1A) from which a  $K_{\text{ox,app}}^{\text{Im}}$  of  $24 \pm 3 \mu\text{M}$  was obtained. Insert: Visible spectra (absorbance versus wavelength in nanometers) of His117Gly azurin with increasing concentrations of imidazole (0, 18, 36, 57, 90, 145, 223, 396, and 800 mM). The arrows indicate the direction of the observed changes upon increasing the imidazole concentration.

nm.<sup>34</sup> The extinction coefficients and Cu dissociation constants were determined by titrating apo-His117Gly azurin with  $\text{Cu}(\text{NO}_3)_2$ , as described in Materials and Methods. The extinction coefficients at 420 and 628 nm obtained in this way are  $2.2 \pm 0.1$  and  $1.2 \pm 0.1 \text{ mM}^{-1}\text{cm}^{-1}$ , respectively, while the Cu dissociation constant for His117Gly azurin without external ligands was determined as  $K_d = 0.5 \pm 0.3 \mu\text{M}$ .

The extinction coefficient of the H117G/Im complex azurin at 628 nm was measured by titration of apo-His117Gly azurin with  $\text{Cu}(\text{NO}_3)_2$  in the presence of excess imidazole (see Materials and Methods) and a value  $\epsilon_{628}^{\text{Im}} = 5.3 \pm 0.1 \text{ mM}^{-1}\text{cm}^{-1}$  was determined.

Figure 1 shows the changes in the UV-vis spectrum that are observed upon addition of imidazole to a solution of oxidized holo His117Gly azurin, as a function of the total amount of added imidazole. The absorption band at 420 nm decreases in intensity while the band at 628 nm increases. Figure 1 also shows the fit to equation 1A, from which the apparent dissociation constant ( $K_{\text{ox,app}}^{\text{Im}}$ ) of  $24 \pm 3 \mu\text{M}$  was determined. Since imidazole has a  $\text{p}K_a$  of 6.95,<sup>31</sup> most of it is protonated at the pH at which these experiments were performed (pH 6.0). After correcting for this protonation equilibrium using eq. 1B the dissociation constant,  $K_{\text{ox}}^{\text{Im}} = 2.4 \pm 0.3 \mu\text{M}$ . Similar experiments with chloride gave  $K_{\text{ox}}^{\text{Cl}} = 16 \pm 2 \text{ mM}$  and an absorbance maximum at 648 nm with an  $\epsilon_{648}^{\text{Cl}} = 6.1 \pm 0.1 \text{ mM}^{-1}\text{cm}^{-1}$ .

**Electrochemistry.** Figure 2 shows examples of potentiometric titrations and their fits. In the absence of external ligands (Figure 2A), His117Gly azurin has a remarkably high reduction (midpoint) potential ( $E^0$ ) of  $670 \pm 10 \text{ mV}$  as compared to 335 mV of *wt* azurin at pH 6.0.<sup>35</sup> Owing to instability, relatively few points could be measured at potentials above 700 mV, which corresponds to  $> 70\%$  oxidation. In the presence of 1.0 M chloride, pH 6, (Figure 2B) the reduction potential decreases to  $574 \pm 5 \text{ mV}$ .

Figure 3 shows the reduction potentials of His117Gly azurin in the presence of four different concentrations of imidazole

(34) Resonance Raman studies have shown that in the absence of external ligands two different species are present at pH 6.0 in an unknown ratio (see ref 17). For the fitting procedure, however, the His117Gly azurin species can be treated adequately as a single species.

(35) van Pouderoyen, G.; Mazumdar, S.; Hunt, N. I.; Hill, A. O.; Canters, G. W. *Eur. J. Biochem.* **1994**, *222*, 583–588.

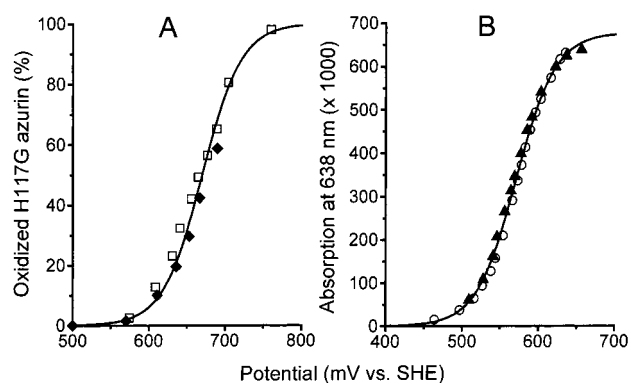


**Figure 2.** Potentiometric titration of His117Gly azurin ( $\sim 0.1 \text{ mM}$ , 20 mM MES, pH 6.0, 33 mM  $\text{Na}_2\text{SO}_4$ , 20 °C); (A) in the absence of external ligands. The two sets of points measured during stepwise reduction ( $\square$ ,  $\blacklozenge$ ) result from two separate titrations. To be able to compare the experiments with each other, the data points from both titrations were normalized against total protein concentration; (B) in the presence of 1.0 M NaCl. Data points were measured during stepwise reduction ( $\circ$ ) and stepwise reoxidation ( $\blacktriangle$ ). The lines are least-squares fits of the data points to the Nernst equation ( $E^0 = 670 \text{ mV}$  (A),  $E^0 = 574 \text{ mV}$  (B)). Potentials are given vs SHE.

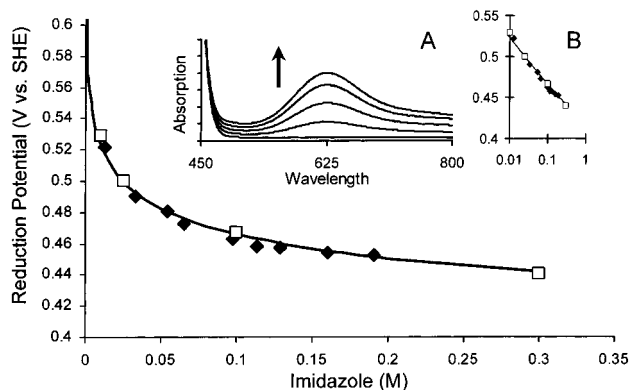
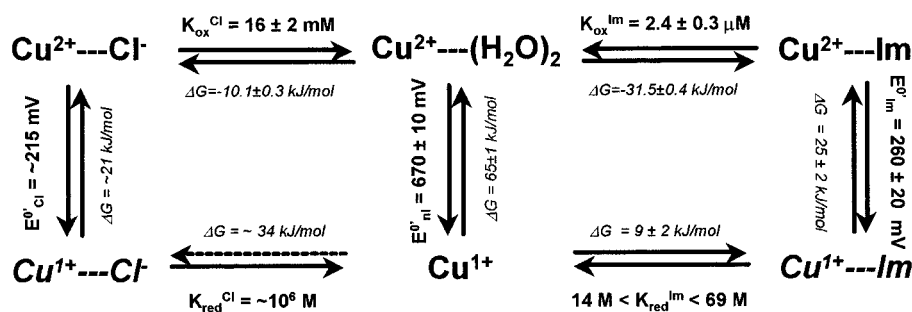


**Figure 3.** Reduction potentials of His117Gly azurin (0.1–0.2 mM in 20 mM MES, pH 6.0, 20 °C) in the presence of increasing concentrations of imidazole. Open squares ( $\square$ ) and closed diamonds ( $\blacklozenge$ ) denote points determined by potentiometric titrations and by imidazole titrations of His117Gly azurin in a “redox-buffer”, respectively (see text). The line shows the simulation using eq 2 ( $E^0_{\text{nl}} = 670 \text{ mV}$ ,  $K_{\text{ox,app}}^{\text{Im}} = 24 \mu\text{M}$ ,  $K_{\text{red,app}}^{\text{Im}} > 1 \text{ M}$ ). (Insert A) Optical spectra (absorbance versus wavelength in nanometers) of His117Gly azurin in a “redox-buffer” ( $\sim 420 \text{ mV}$ , see text) as a function of increasing concentration of imidazole (0, 33, 66, 98, and 129 mM). The arrow denotes the direction of the changes when the imidazole concentration is increased. (Insert B) Same data as in the main graph but with the abscissa plotted on a logarithmic scale.

(10, 25, 100, and 300 mM) as determined by separate potentiometric titrations (open squares). In a second experiment, a solution of His117Gly azurin, “redox buffered” at 420 mV, was titrated with imidazole (data shown as black diamonds). At low imidazole concentrations, no detectable amount of oxidized protein is observed because of the high reduction potential of His117Gly azurin, but as the concentration of imidazole is raised the reduction potential decreases and His117Gly azurin is progressively oxidized. This is observed spectroscopically (Figure 3, insert A). The spectroscopically determined concentration of oxidized His117Gly azurin was used to calculate the reduction potentials of His117Gly azurin at the different imidazole concentrations. High imidazole concentrations caused leaching of the Cu from the active site, so the formal reduction potential,  $E^0(\text{Im})$  of the His117Gly/Im system could not be determined accurately at  $[\text{Im}] > 0.3 \text{ M}$ . In the range for which

## Scheme 1



the reduction potential could be determined, a logarithmic dependence on the imidazole concentration ( $-60 \pm 2 \text{ mV}/\log [\text{Im}]$ ) was observed (Figure 3, insert B). The dependence of potential on the imidazole concentration is a direct consequence of the difference in dissociation constants of the reduced and oxidized His117Gly/Im, that is,  $K_{\text{red}}^{\text{Im}}$  and  $K_{\text{ox}}^{\text{Im}}$  (see Theory section, eqs 2 and 3).

Analysis of the data on the basis of eq 3 shows that even at 300 mM total imidazole, which is the highest concentration that could be used without incurring Cu depletion, the ligand concentration is still much lower than the dissociation constant for the reduced copper site (i.e.  $[\text{Im}]_t \ll K_{\text{red}}^{\text{Im,app}}$ ). Therefore, only a lower limit for  $K_{\text{red}}^{\text{Im,app}}$  ( $> 1 \text{ M}$ ) could be assessed on the basis of these experiments. From eqs 1B and 2 it follows that  $K_{\text{red}}^{\text{Im}} > 0.1 \text{ M}$  and  $E_{\text{Im}}^0 < 400 \text{ mV}$ , the latter being the reduction potential at infinite imidazole concentration.

The data can be incorporated into a thermodynamic scheme as shown in Scheme 1, in which the species that have virtually zero concentration are shown in italics. The details of this scheme will be discussed in the next section.

**Fast-Scan Protein-Film Voltammetry.** With a relatively slow technique like potentiometry it is not possible to determine the formal reduction potential of the His117Gly/Im complex ( $E_{\text{Im}}^0$ ) because the concentrations of imidazole required to coordinate the reduced Cu(I) are so high as to cause Cu depletion. Even higher concentrations were found to be required in the case of  $\text{Cl}^-$  (vide infra). Cyclic voltammetry on adsorbed protein films provides a solution to this problem, since the use of fast scan rates or low temperatures makes it possible to trap transient species and to measure their reduction potentials and kinetics.<sup>23,28,36</sup> Thus, efforts were focused next upon characterizing the thermodynamic and kinetic properties of the Cu/ligand complexes by using fast-scan protein-film voltammetry.

Figure 4 shows background-corrected voltammograms of His117Gly azurin adsorbed on a PGE electrode that is immersed in a solution containing 250 mM imidazole at 0 °C (left) or 0.5 M  $\text{Cl}^-$  at 20 °C (right). The voltammograms, which are initial cycles commenced from an oxidative poise, were recorded over a range of scan rates.

At low scan rates the voltammograms appear quite simple and reversible (Figure 4A and 4D), although even at 10  $\text{mV s}^{-1}$  the systems are not completely ideal. The peak separations in either case (40–50 mV) at low scan rates are higher than for *wt* azurin ( $\sim 10 \text{ mV}$ ) and average half-height peak widths are around 110–130 mV (although note that the oxidative peaks are relatively narrow, particularly with  $\text{Cl}^-$  as ligand). By contrast, peak widths obtained for *wt* azurin (90–100 mV) lie closer to the theoretical value (83 mV at 0 °C).<sup>37</sup> These

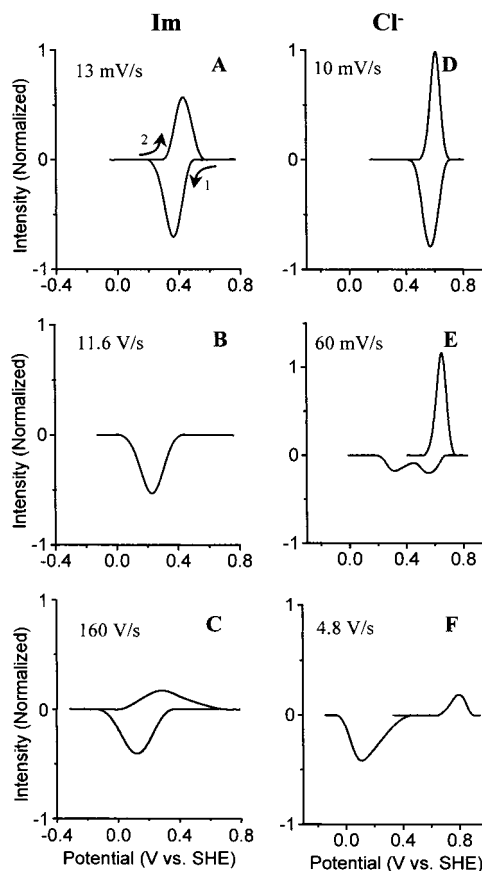


**Figure 4.** Baseline-corrected and normalized voltammograms at different scan rates of His117Gly azurin films in (A, B, C) 250 mM imidazole (0 °C, 20 mM MES/ $\text{H}_2\text{SO}_4$  pH 6.0, 150 mM  $\text{Na}_2\text{SO}_4$ ) and (D, E, F) 0.5 M  $\text{NaCl}$  (20 °C, 20 mM MES pH 6.0). Arrows and numbers shown in (A) indicate direction and origin of cycles.

deviations are suggestive of competing coupling processes, and this was indeed confirmed by increasing the scan rate. We will describe the results recorded with imidazole and chloride separately.

**Imidazole.** For scan rates in the region of  $10 \text{ V s}^{-1}$ , with the cycle commenced from an oxidative poise, the oxidative peak disappears whereas a broadened reductive peak is retained (Figure 4B), while at scan rates above  $50 \text{ V s}^{-1}$  a broad oxidative peak reappears (Figure 4C). The disappearance of the oxidative peak in this region of scan rate suggests that the reoxidation reaction is “gated” by a preceding step. Specifically, reduction of His117Gly azurin is followed rapidly by dissociation of the imidazole; if this results in a form that is redox inactive (either because of intrinsically slow electron-transfer kinetics or a high reduction potential) the reoxidation reaction cannot occur unless imidazole becomes re-coordinated. However, at scan rates above  $50 \text{ V s}^{-1}$  the oxidative peak reappears, because at these scan

(36) Armstrong, F. A.; Heering, H. A.; Hirst, J. *Chem. Soc. Rev.* **1997**, 26, 169–179.

(37) Laviron, E. In *Electroanalytical Chemistry*; Bard, A. J., Eds.; Marcel Dekker: New York, 1982; Vol. 12, pp 53–157.

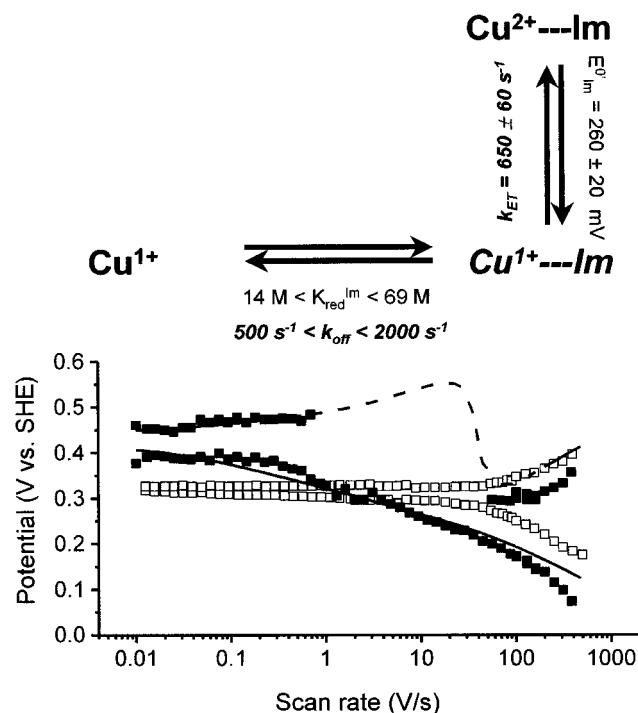


**Figure 5.** Peak positions (vs SHE) in the voltammograms (see Figure 4 A, B, and C) of His117Gly azurin (closed symbols, ■) and *wt* azurin (open symbols, □) as a function of scan rate (0 °C, 20 mM MES pH 6.0, 150 mM Na<sub>2</sub>SO<sub>4</sub>). The line represents the simulation using the model at the top of the picture, with  $k_{\text{on}} = 4 \text{ s}^{-1}$ ,  $k_{\text{off}} = 850 \text{ s}^{-1}$  (thus  $K_{\text{red,app}}^{\text{Im}} = 213 \text{ M}$ ),  $E_{\text{Im}}^0 = 260 \text{ mV}$  and an electron-transfer rate ( $k_0$ ) of  $650 \text{ s}^{-1}$ . The simulation includes the addition of a constant peak-separation of 33 mV. The broken line indicates where in the simulation the peak height was less than 10% of that at  $10 \text{ mV s}^{-1}$ . “Cu<sup>1+</sup>” and “Cu<sup>2+</sup>” represent Cu(I)His117Gly and Cu(II)His117Gly azurin, respectively.

rates the His117Gly azurin/imidazole complex is reoxidized before dissociation occurs, that is, the imidazole is “trapped” in the protein.

Voltammograms commenced from a reductive poise (data not shown) resemble those for the oxidative poise provided the scan rate is below  $50 \text{ V s}^{-1}$ . However, at scan rates  $> 50 \text{ V s}^{-1}$  no signals were observed in either direction. This is as expected, since if one starts from reduced His117Gly azurin, which has no imidazole coordinated and thus is redox-inactive, the potential cycle is completed before imidazole can enter the copper site.

Figure 5 shows how the peak positions vary with scan rate, and includes, for comparison, the data for *wt* azurin (open symbols) measured under the same conditions. As evinced by the small peak separation, which increases only as the scan rates approach  $100 \text{ V s}^{-1}$ , *wt* azurin shows remarkably fast electron transfer.<sup>23</sup> It is immediately clear also that the behavior of His117Gly azurin in the presence of imidazole is far more complicated. At low scan rates, the reduction potential (which is dependent on imidazole concentration) remains fairly constant until the oxidative peak disappears. At high scan rates ( $> 50 \text{ V s}^{-1}$ ) a broad oxidative peak reappears as the imidazole ligand is trapped in the Cu(I) state and a reversible redox couple emerges with a reduction potential that is just 50–80 mV lower than  $E^0$  for *wt* azurin (pH 6.0). Since the peaks at scan rates  $> 50 \text{ V s}^{-1}$  are relatively broad, an accurate peak maximum is difficult to obtain, and general errors of  $\pm 10 \text{ mV}$  for these data points have to be taken into account.

Figure 5 includes the fits obtained using Scheme 1 and the kinetic model shown at the top of the figure, in which the ligand

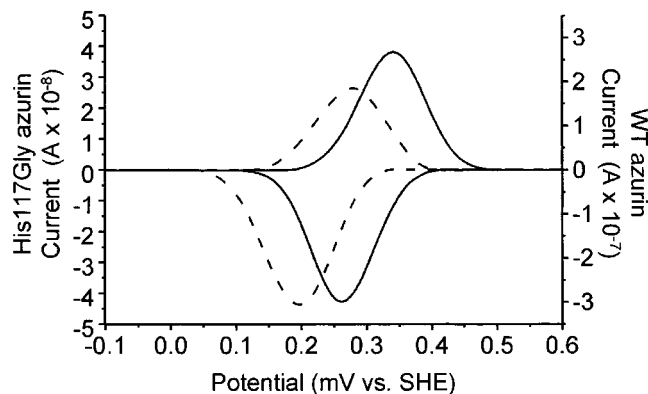


**Figure 6.** Baseline corrected voltammograms of *wt* (solid line) and His117Gly (dashed line) azurin with 5 mM imidazole at  $100 \text{ mV s}^{-1}$  at  $-70 \text{ }^\circ\text{C}$  (70% MeOH, 20 mM MES pH\* = 6.0, 0.1 M NaClO<sub>4</sub>). The current scales have been adjusted to show approximately equal signal amplitudes.

binding rates and the electron-transfer kinetics were analyzed with a finite difference procedure.<sup>28,38</sup> The electron-transfer kinetics were modeled using the Butler–Volmer equation.<sup>39</sup> The simulations show that the electron-transfer rate constant ( $k_0$ ) of His117Gly azurin complexed with imidazole ( $650 \pm 60 \text{ s}^{-1}$ ) is of the same order of magnitude as that of *wt* azurin ( $2000 \pm 200 \text{ s}^{-1}$ ). At the temperature studied (0 °C)  $K_{\text{red,app}}^{\text{Im}}$  lies between 100 and 500 M. The rate constant for  $k_{\text{off}}$  lies between 500 and 2000  $\text{s}^{-1}$ , while  $k_{\text{on}}$  is between 2 and 10  $\text{M}^{-1} \text{ s}^{-1}$  (the rates are interdependent, and their ratio must be within the range given for  $K_{\text{red,app}}^{\text{Im}}$ ). The corresponding value of  $E_{\text{Im}}^0$  lies between 242 and 280 mV, whereas *wt* azurin has  $E^0 = 330 \pm 5 \text{ mV}$  under these conditions (250 mM imidazole/H<sub>2</sub>SO<sub>4</sub>, pH 6.0, 150 mM Na<sub>2</sub>SO<sub>4</sub>, 0 °C). With an average value of  $E_{\text{Im}}^0 = 260 \pm 20 \text{ mV}$  at 0 °C, and using the room-temperature values of  $E_{\text{nl}}^0$  (670 mV) and  $K_{\text{ox,app}}^{\text{Im}}$  (24  $\mu\text{M}$ ),  $K_{\text{red,app}}^{\text{Im}}$  is determined to lie in the range  $140 \text{ M} < K_{\text{red,app}}^{\text{Im}} < 680 \text{ M}$ , in broad agreement with the range of  $100 \text{ M} < K_{\text{red,app}}^{\text{Im}} < 500 \text{ M}$  derived above. Correcting the apparent dissociation constants for the protonation reaction of imidazole (see Theory) results in  $14 \text{ M} < K_{\text{red}}^{\text{Im}} < 69 \text{ M}$ . The large errors arise from uncertainties in measuring the peak positions at high scan rate.

To make further comparisons between *wt* and His117Gly azurins, protein film cyclic voltammograms were measured at  $-70 \text{ }^\circ\text{C}$ , using 70% methanol in water as a cryosolvent.<sup>22</sup> At this temperature the imidazole could be trapped in the Cu(I) state at much lower scan rates ( $\leq 100 \text{ mV s}^{-1}$ ). The baseline-corrected voltammograms of His117Gly azurin and *wt* azurin are presented in Figure 6 and reveal two important points. First, His117Gly azurin with imidazole shows a reversible response

(38) Britz, D. *Digital Simulation in Electrochemistry*; Springer-Verlag: Berlin, 1988.

(39) For modest peak separation (until  $\sim 300 \text{ mV}$ ) the use of the “simpler” Butler–Volmer equation instead of the Marcus equation can be justified. See for instance ref 23 and Honeychurch, M. J. *Langmuir* **1999**, *15*, 5158–5163.

(40) While the difference between the reduction potentials of *wt* and His117Gly azurin at  $-70 \text{ }^\circ\text{C}$  corresponds well with the difference observed at 0 °C, the absolute values are unexpected. This is because the *wt* potential in methanolic buffer at 0 °C is 321 mV, and lowering the temperature should increase  $E^0$ , in line with the negative entropy of reduction. See ref 50. The slight decrease is attributed partly to an increase in pH\* as the temperature is lowered (extrapolation of pH measurements from results obtained at temperatures  $> 0 \text{ }^\circ\text{C}$  show that the pH\* increases from 6.0 at 0 °C to 7.0 at  $-70 \text{ }^\circ\text{C}$ ). The reduction potential of *wt* azurin at 25 °C is shown to decrease by  $\sim 23 \text{ mV}$  going from pH 6.0 to 7.0. See ref 35. Some contribution may also arise from our use of NaClO<sub>4</sub> electrolyte, which is reported to display unusual chaotropic properties. See: Battistuzzi, G.; Borsari, M.; Loschi, L.; Sola, M. *J. Biol. Inorg. Chem.* **1997**, *2*, 350–359.



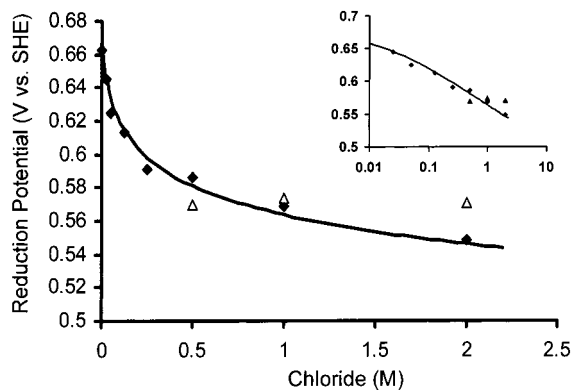


**Figure 7.** Reduction potentials of His117Gly azurin (20 mM MES, pH 6.0, 20 °C) in the presence of increasing concentrations of chloride. Triangles ( $\Delta$ ) and diamonds ( $\blacklozenge$ ) denote points determined by potentiometric titrations and by cyclic voltammetry (scan rate 1 mV s<sup>-1</sup>). The line shows the simulation using eq 2 ( $E_{nl}^{0'} = 670$  mV,  $K_{ox}^{Cl} = 16$  mM,  $K_{red}^{Cl} > 5$  M). Insert B: Same data as in the main graph but with the abscissa plotted on a logarithmic scale.

that is similar to *wt* azurin, and second, the  $E_{lm}^{0'}$  value of His117Gly azurin is 62 mV less than that of *wt* azurin (236 mV vs 298 mV).<sup>40</sup>

**Chloride.** As depicted in Figure 7, the reduction potentials obtained from cyclic voltammograms recorded at sufficiently slow scan rates (i.e., 1 mV s<sup>-1</sup>) show a logarithmic dependence on Cl<sup>-</sup> concentration (black diamonds in Figure 7), similar to that observed for imidazole. The concentration behavior could be simulated with eq 2 in which Im had been replaced by Cl<sup>-</sup>, using  $K_{ox}^{Cl} = 16$  mM and  $E_{nl}^{0'} = 670$  mV (solid line in Figure 7). There is reasonable agreement with a limited amount of solution potentiometric data (triangles in Figure 7), although for reasons that we do not understand, the latter experiments did not show any decrease in potential above 0.5 M Cl<sup>-</sup>.<sup>41</sup>

At scan rates above 10 mV s<sup>-1</sup>, the voltammograms measured for His117Gly azurin in 0.5 M Cl<sup>-</sup> (Figure 4E and 4F) display different behavior compared to those measured in 250 mM imidazole (Figure 4B and 4C). In the region between 30 and 100 mV s<sup>-1</sup> (Figure 4E) a second reductive peak appears at lower potentials and replaces the single peak observed at scan rates <30 mV s<sup>-1</sup>. At scan rates above 100 mV s<sup>-1</sup> (Figure 4F) both the new reducing and the oxidizing signal separate until they disappear at around 10 V s<sup>-1</sup>. Although at these high scan rates it was difficult to measure the amplitude of the observed signals accurately, the peak positions were reliable within  $\pm 10$  mV. No new signals appear as the scan rate is raised to 100 V s<sup>-1</sup>. The voltammogram at 4.8 V s<sup>-1</sup> has a large peak separation, but this is not due to slow electrode kinetics, rather it is the result of the coupling of electron transfer to fast ligand exchange. The peak maxima of the voltammograms at increasing Cl<sup>-</sup> concentration are also depicted in Figure 8.

As with imidazole, the results can be explained in terms of rapid dissociation of Cl<sup>-</sup> from the Cu(I) state, but now it is necessary to include the rate of Cl<sup>-</sup> dissociation from Cu(II)

(41) In contrast to the model shown in Scheme 1, the potentiometric titrations at three different Cl<sup>-</sup> concentrations showed  $E_{nl}^{0'}(Cl)$  values which are equal within the experimental error. These experiments at high Cl<sup>-</sup> concentration (0.5 M < [Cl<sup>-</sup>] < 2.0 M) are however problematic due to substantial changes in the ionic strength and uncertainties in the liquid junction of the reference electrode. Further complications might derive from the slow kinetics which are found for some of the reactions on the left-hand square of Scheme 1, like  $k_{off}$  for oxidized H117G/Cl (0.3 s<sup>-1</sup>), the electron-transfer rates ( $k_0 \approx 10$  s<sup>-1</sup>) and an undetectably slow  $k_{on}$  of Cl<sup>-</sup> for the reduced His117Gly azurin. These slow kinetics could result in measurements which do not represent equilibrium situations.

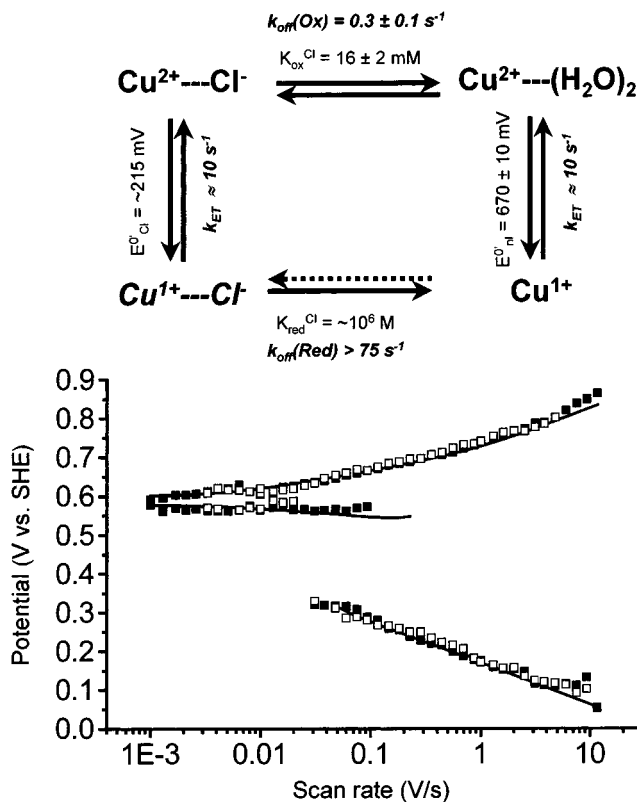


**Figure 8.** Peak positions (vs SHE) in the voltammograms (see Figure 4D, E and F) of His117Gly azurin in 0.5 M NaCl as a function of scan rate (20 °C, 20 mM MES pH 6.0) starting from an oxidative poise (closed symbols,  $\blacksquare$ ) and from a reductive poise (open symbols,  $\square$ ). The line represents the simulation using the model at the top of the picture, with  $k_{off}(Ox) = 0.3$  s<sup>-1</sup>,  $k_{off}(Red) = 200$  s<sup>-1</sup>,  $E_{nl}^{0'} = 670$  mV,  $E_{Cl}^{0'} = 215$  mV and electron-transfer rates ( $k_0$ ) of 10 s<sup>-1</sup> for both species. The simulation includes the addition of a constant peak-separation of 20 mV. “Cu<sup>1+</sup>” and “Cu<sup>2+</sup>” represent Cu(I)His117Gly and Cu(II)His117Gly azurin, respectively.

which is relatively fast compared to that of imidazole. Thus, reduction of the Cu(II) state can occur either directly (at low potential) to give the unstable Cu(I)–Cl<sup>-</sup> form, or electron transfer at higher potential can follow the dissociation of Cl<sup>-</sup>. The two pathways give rise to the two reduction peaks observed at scan rates between 30 and 110 mV s<sup>-1</sup>. As the scan rate is raised further, dissociation of Cl<sup>-</sup> from Cu(II) is unable to compete with the rate of change in potential and just one reduction peak is observed. Since *reduced* H117G/Cl complex rapidly dissociates, and reassociation is very unfavorable, His117Gly azurin is only reoxidized at the high potential of the unliganded form. Due to the high rate of ligand dissociation from Cu(I), scans commencing from a reductive poise are similar to those commencing from an oxidative poise.

Figure 8 includes the fit obtained with a finite difference procedure based on a model that is shown as an insert. The simulations show that Cl<sup>-</sup> dissociates from *oxidized* His117Gly azurin with a rate constant ( $k_{off}(Ox) = 0.3 \pm 0.1$  s<sup>-1</sup>). For the dissociation of Cl<sup>-</sup> from the *reduced* His117Gly azurin, only a limiting rate for Cl<sup>-</sup> dissociation could be derived ( $k_{off}(Red) > 75$  s<sup>-1</sup>). Since a single reversible redox couple could not be isolated, it was not possible to obtain electron-transfer rates ( $k_0$ ) for H117G or H117G/Cl. For the same reason, the reduction potential of the H117G/Cl species ( $E_{Cl}^{0'}$ ) could not be measured directly. The simulations showed however that in either case (i.e. with and without Cl<sup>-</sup>)  $k_0$  must be slow, that is, of the order of just 10 s<sup>-1</sup>. This accords with the results obtained for

His117Gly azurin in the presence of imidazole, in which the uncomplexed His117Gly azurin gave no oxidation peak. Finally, the simulation showed that  $E^{\circ}_{\text{Cl}}$  is even lower than  $E^{\circ}_{\text{Im}}$  with an approximate value of 215 mV.

## Discussion

Replacing the copper-coordinating His117 of azurin by a glycine creates a copper site that is accessible for external ligands.<sup>17,18</sup> We have now determined the thermodynamic and kinetic properties of two systems having exchanging ligands, that is, chloride—a simple ligand—and imidazole, which offers the possibility of restoring the native coordination sphere.

The left-hand part of Scheme 1 is relevant when chloride is present in solution. Several items of evidence support the represented equilibria. (a) From a recent combined EXAFS and NMR study of His117Gly azurin in the absence and presence of ligands such as imidazole (20 mM) and chloride (0.5 M)<sup>42</sup> it was concluded that the presence of  $\text{Cl}^-$  within 6 Å of the Cu(I) could be ruled out, that is, at this concentration  $\text{Cl}^-$  is not coordinated to Cu(I). (b) Cyclic voltammetry at slow scan rates (1 mV  $\text{s}^{-1}$ ) shows that the reduction potential decreases with increasing  $\text{Cl}^-$  concentration in a Nernstian manner even above 1 M concentration, consistent with a low affinity of  $\text{Cl}^-$  for the reduced copper site ( $K_{\text{red}}^{\text{Cl}} \gg [\text{Cl}^-]$ ). (c) Fast scan cyclic voltammetry reveals a dynamic system, in which the reduced H117G/ $\text{Cl}^-$  is very rapidly dissociated, while its association is too slow to be observed directly. On the basis of these experiments, some estimates may be made. First, electron transfer for both uncomplexed H117G and the H117G/ $\text{Cl}^-$  complex is slow ( $k_0 \approx 10 \text{ s}^{-1}$ ). Second, the reduction potential of H117G/ $\text{Cl}^-$  is  $\sim 215$  mV. By using this value and completing the left-hand square of Scheme 1, the dissociation constant of the reduced H117G/ $\text{Cl}^-$  complex,  $K_{\text{red}}^{\text{Cl}}$  is estimated to be around  $10^6$  M, that is, an impossibly high concentration would be required to occupy the coordination site. In other words, the chloride ion is strongly repelled from the reduced copper site.

There are at least two reasons why electron transfer in native azurin and in the complex with imidazole is more efficient than when His117 is replaced by  $\text{Cl}^-$  or  $\text{H}_2\text{O}$ . First, replacing an imidazole group by  $\text{Cl}^-$  or  $\text{H}_2\text{O}$  creates a site with a higher reorganization energy. Second, the loss of the imidazole ring destroys the electronic coupling between the copper atom and the redox partner. As has been suggested before,<sup>35,43–48</sup> the imidazole ring of His117 provides an excellent pathway for the electron to transfer to external partners or, in this case, the electrode.

For the His117Gly azurin/imidazole complex, trapped at high scan rates or low temperature, that is,  $-70$  °C in 70% methanol, the cyclic voltammetry experiments show that  $E^{\circ}$  is only  $\sim 60$  mV lower than  $E^{\circ}$  for *wt* azurin. Aside from this difference, the His117Gly/imidazole redox couple behaves in a manner that is remarkably similar to *wt* azurin. It seems unlikely that the difference in  $E^{\circ}$  results from a change in the copper site geometry, since oxidized His117Gly azurin with imidazole is

spectroscopically very similar to *wt* azurin.<sup>17,18,21,42</sup> However, the His117Gly mutation may have loosened the protein structure slightly in the neighborhood of the mutation and consequently increased the solvent accessibility of the copper site.<sup>49</sup>

The data shown in the right-hand part of Scheme 1 may now be commented upon. In the absence of external ligands, and at 20 °C, His117Gly azurin exhibits a high reduction potential ( $670 \pm 10$  mV), whereas the reduction potential of the His117Gly/Im complex, albeit measured at a different temperature (0 °C), is just 260 mV.<sup>50</sup> This shift of 410 mV corresponds to a difference in the dissociation constants for oxidized and reduced His117Gly/Im of 7 orders of magnitude ( $K_{\text{ox}}^{\text{Im}} = 2.4 \pm 0.3 \mu\text{M}$ ;  $14 < K_{\text{red}}^{\text{Im}} < 69$  M). In other words the Cu(I) state has very little affinity for imidazole. These estimates of  $K_{\text{red}}^{\text{Im}}$  and  $E^{\circ}_{\text{Im}}$  are in agreement with the lower and upper limits calculated on the basis of ligand and potentiometric titrations on protein solutions at 20 °C, respectively.

These results are conspicuously similar to the behavior of pseudoazurin, plastocyanin, and amicyanin. When these blue copper proteins are reduced, the C-terminal histidine can dissociate from the Cu and protonate, with  $\text{pK}_a$ 's in the range from 4 to 7.5.<sup>51–56</sup> Crystal structures show that Cu(I) is displaced toward the plane of the remaining ligands ( $\text{S}^{\gamma}$  of the Cys,  $\text{N}^{\delta}$  of the His and  $\text{S}^{\delta}$  of the Met).<sup>6,10</sup> Like His117Gly azurin, these proteins exhibit high reduction potentials when the copper is in its three-coordinated form.<sup>14,16</sup>

The dissociation constant for reduced H117G/Im ( $K_{\text{red}}^{\text{Im}}$ ) lies between 14 and 69 M. One might ask what the dissociation constant would be for His117 in the reduced *wt* azurin. In the latter case the dissociation of His117 is intramolecular while with the His117Gly azurin variant, the dissociation/association of the imidazole is intermolecular and the equilibrium constant involves the concentration of imidazole in solution. It has been argued<sup>57</sup> that an association reaction in which the two reaction partners are present on the same framework (in our case, the protein) favors complex formation by an entropic term that is equivalent to a concentration of  $6 \times 10^9$  M in one of the components. Since the intermolecular  $K_d$  for dissociation of the H117G/Im complex lies in the range 14–69 M, the corresponding intramolecular  $K_d$  in *wt* azurin would amount to  $(2–11) \times 10^{-9}$ . Allowance for some rotational entropy of the His117 side chain in its dissociated state that would partially cancel the effect of the high internal “effective concentration” and could increase  $K_d$  by up to 3 orders of magnitude,<sup>57</sup> leads, finally, to an estimated maximal  $K_d$  of  $10^{-6}$ . Knowing the  $\text{pK}_a$  of His117 in apo *wt* azurin to be 7.7 in  $\text{D}_2\text{O}$ ,<sup>58</sup> the  $\text{pK}_a$  in the reduced holo protein is calculated to be lower than 2 (see eq 1B). From these

(49) Increased solvent accessibility is expected to lower the reduction potential for positively charged copper sites such as in azurin. See: Churg, A. K.; Warshel, A. *Biochemistry* **1986**, *25*, 1675–1681; Tezcan, F. A.; Winkler, J. R.; Gray, H. B. *J. Am. Chem. Soc.* **1998**, *120*, 13383–13388.

(50) Battistuzzi, G.; Borsari, M.; Loschi, L.; Righi, F.; Sola, M. *J. Am. Chem. Soc.* **1999**, *121*, 501–506.

(51) Dennison, C.; Kohzuma, T.; McFarlane, W.; Suzuki, S.; Sykes, A. G. *Inorg. Chem.* **1994**, *33*, 3299–3305.

(52) Dennison, C.; Kohzuma, T.; McFarlane, W.; Suzuki, S.; Sykes, A. G. *J. Chem. Soc., Chem. Commun.* **1994**, 581–582.

(53) Dennison, C.; Vijgenboom, E.; Hagen, W. R.; Canters, G. W. *J. Am. Chem. Soc.* **1996**, *118*, 7406–7407.

(54) Lommen, A.; Canters, G. W.; van Beeumen, J. *Eur. J. Biochem.* **1988**, *176*, 213–223.

(55) Segal, M. G.; Sykes, A. G. *J. Am. Chem. Soc.* **1978**, *100*, 4585–4592.

(56) Zhu, Z. Y.; Cunane, L. M.; Chen, Z. W.; Durley, R. C. E.; Mathews, F. S.; Davidson, V. L. *Biochemistry* **1998**, *37*, 17128–17136.

(57) Fersht, A. *Enzyme Structure and Mechanism*; W. H. Freeman and Company: New York, 1985; pp 56–63.

(58) van de Kamp, M.; Hali, F. C.; Rosato, N.; Agro, A. F.; Canters, G. W. *Biochim. Biophys. Acta* **1990**, *1019*, 283–292.

(42) Jeuken, L. J. C.; Ubbink, M.; Bitter, J. H.; van Vliet, P.; Meyer-Klaucke, W.; Canters, G. W. *J. Mol. Biol.* **2000**, *299*, 737–755.

(43) Adman, E. T. *Adv. Protein Chem.* **1991**, *42*, 144–197.

(44) Brooks, H. B.; Davidson, V. L. *Biochemistry* **1994**, *33*, 5696–5701.

(45) Buning, C.; Canters, G. W.; Comba, P.; Dennison, C.; Jeuken, L.; Melter, M.; Sanders-Loehr, J. *J. Am. Chem. Soc.* **2000**, *122*, 204–211.

(46) Chen, L.; Durley, R. C.; Poliks, B. J.; Hamada, K.; Chen, Z.; Mathews, F. S.; Davidson, V. L.; Satow, Y.; Huizinga, E.; Vellieux, F. M. *Biochemistry* **1992**, *31*, 4959–4964.

(47) Kukimoto, M.; Nishiyama, M.; Ohnuki, T.; Turley, S.; Adman, E. T.; Horinouchi, S.; Beppu, T. *Protein Eng.* **1995**, *8*, 153–158.

(48) Ubbink, M.; Ejdeback, M.; Karlsson, B. G.; Bendall, D. S. *Structure* **1998**, *6*, 323–335.



values it is now evident why dissociation of His117 is not observed in *wt* azurins.

### Concluding Remarks

Previously, it has been shown that imidazole restores the spectroscopic properties of *wt* azurin in His117Gly azurin. The work reported here shows that imidazole coordination to the copper in His117Gly is also able to restore, almost completely, the capacity of the native protein for fast electron-transfer. This is in contrast to the external ligands  $\text{Cl}^-$  and  $\text{H}_2\text{O}$ , for which substantially slower electron-transfer rates are determined. This underlines the importance of the blue copper protein structure and its suitability for rapid electron transfer. The previously reported "redox inactivity" of His117Gly azurin is the consequence of the low affinity that its reduced copper site exhibits for external ligands.

Unlike the blue copper proteins amicyanin, plastocyanin, and pseudoazurin, the C-terminal histidine in *wt* azurin does not protonate. In discussing the possible causes for this difference the relative stabilities of the two forms of the Cu center must be taken into account, that is, the form in which the His side chain is coordinated to the Cu and the form in which the His has dissociated from the Cu and has become protonated. First, the Cu(I)–His117 bond might be stronger in azurin than the analogous bonds in plastocyanin, amicyanin, and pseudoazurin. However, for the spectroscopically more accessible Cu(II) form there is no indication from UV–vis, EPR, and resonance Raman data for a stronger Cu–His bond in azurin than in the other proteins, and this is likely to hold for the reduced forms as well. Second, the dissociation of the His might be favored because in its dissociated form the His might be able to form more H-bonds. This requires further investigation of the hydrogen-bonding pattern around the Cu site in the various blue copper proteins. Research in this direction is underway. Third, the protein framework around the Cu site might be less rigid in the other blue copper proteins than in azurin. This could favor His dissociation. A thorough NMR relaxation study might shed light on this possibility. The NMR evidence available so far shows that the mobility of the ligand loop in azurin can be enhanced by point or loop mutations and the question is if dissociation of His117 would be equivalent in this respect to a point mutation. A systematic study of the effect on protein mobility of replacing His117 by smaller side chains might shed light on this question.<sup>59</sup> An interesting case in point is provided by the crystal structure of the Met121Gln azurin variant, where in the

reduced form the copper ion moves away from His117 resulting in a Cu–N<sup>δ</sup> distance of 2.67 Å.<sup>60</sup> Although, at this distance the binding is expected to be very weak, the histidine can still not be protonated.<sup>61</sup> Finally, it has been suggested that the structure and the number of residues in the loop containing the copper-coordinating and surface-exposed histidine might have an effect on the protonation of this histidine.<sup>51</sup> However, loop mutagenesis studies on amicyanin do not support this suggestion.<sup>53</sup>

It has been pointed out that type-1 copper sites exhibit reduction potentials that are more positive than the Cu(II)/Cu(I) redox couple in water (~150 mV). The inference has been made that the metal binding site in blue copper proteins is tailored to accommodate Cu(I) better than Cu(II), leading to a preferential stabilization of the Cu(I) form. The findings of the present study now enable this idea to be qualified and quantified. Without the histidine ligand, the site greatly favors Cu(I); *with* the histidine, however, the balance is shifted back toward Cu(II). The thermodynamic results displayed in Scheme 1 show that in the Cu(I) form azurin has a strong tendency to *eject* the solvent exposed histidine ligand. It seems, therefore, that the origin of the high reduction potential of blue copper proteins must be sought in causes other than the purported stabilization by the protein of the Cu(I) over the Cu(II) state.

**Acknowledgment.** The authors are grateful to Professor H.C. Freeman (Sydney) for valuable comments on the manuscript and Dr. Judy Hirst for initial help with voltammetric experiments. This work was financially supported by The Netherlands Ministry of Economic Affairs, the Ministry of Education, Culture and Science, and the Ministry of Agriculture, Nature Management and Fishery in the framework of an industrial relevant research program of The Netherlands Association of Biotechnology Centres in The Netherlands (ABON). Research in the laboratory of F.A.A. is supported by the United Kingdom EPSRC and BBSRC (43/B10492 and 43/B11675). R.C. thanks the National Council of Science and Technology of Mexico (CONACYT) for their support.

JA0006144

(59) Canters, G. W.; Kalverda, A. P.; Hoitink, C. W. In *The Chemistry of the Copper and Zinc Triads*; Welch, A. J., Chapman, S. K., Eds.; The Royal Society of Chemistry: Cambridge, 1993; pp 30–37.

(60) Romero, A.; Hoitink, C. W.; Nar, H.; Huber, R.; Messerschmidt, A.; Canters, G. W. *J. Mol. Biol.* **1993**, 229, 1007–1021.

(61) Diederix, R. E. M.; Canters, G. W.; Dennison, C. *Biochemistry* **2000**, 39, 9551–9560.